

# Bias current dependent resistance peaks in NiFe/Ag giant magnetoresistance multilayers

L. S. Kirschenbaum,<sup>a)</sup> C. T. Rogers, and P. D. Beale  
*Condensed Matter Laboratory, Department of Physics, University of Colorado,  
Boulder, Colorado 80309-0390*

S. E. Russek and S. C. Sanders  
*National Institute of Standards and Technology, Boulder, Colorado 80303-3328*

(Received 17 January 1996; accepted for publication 23 March 1996)

We show that thin-film Ni<sub>82</sub>Fe<sub>18</sub>/Ag multilayer structures display multiple peaks in their magnetoresistance curves when biased at current densities above 10<sup>6</sup> A/cm<sup>2</sup>. These peaks appear for annealed and unannealed structures, and their number is correlated with the number of NiFe layers. At high bias currents, the peak positions shift linearly with the internal magnetic field created by the bias current. The peak positions extrapolate to nonzero fields at zero bias currents, providing an upper bound on the magnetic layer-layer coupling strength of  $J_0 \approx 10^{-20}$  J ( $k_B \times 700$  K). The peak positions do not shift with temperature over the range 200–375 K; their widths narrow with increasing temperature. The single-domain magnetic moment  $\mu$  is estimated as 10<sup>-17</sup> J/T (10<sup>6</sup>  $\mu_B$ ) from the peak widths of  $\sim 0.8$  kA/m. © 1996 American Institute of Physics.  
[S0003-6951(96)04322-7]

In this letter we report the observation of a new and useful high current density behavior for NiFe/Ag multilayer devices. Such devices are promising systems for use as giant magnetoresistance (GMR) sensors due to their high sensitivities at low magnetic fields. We observe a magnetoresistance versus magnetic field curve (MR curve) that evolves from a single-peaked curve at low bias to a multi-peaked curve at high bias. Analysis of the positions and shapes of these MR peaks provides a new set of tools for determining the micro-magnetic structure of the multilayers.

Our multilayers are fabricated from Ni<sub>82</sub>Fe<sub>18</sub> (2.0 nm)/Ag (4.4 nm) films grown on Si/SiO<sub>2</sub>/Ta substrates using sputter deposition.<sup>1</sup> Briefly, the films are composed of a 10 nm Ta layer on Si/SiO<sub>2</sub> followed by five, seven, or nine alternating layers of NiFe and Ag with half-layers of Ag on the top and bottom. A 15 nm Ta cap layer completes the stack. The films are photolithographically patterned into 0.7 to 16  $\mu$ m wide stripes with four-terminal geometries. All data presented in this letter were taken on 16  $\mu$ m wide, 10-square and 8  $\mu$ m wide, 20-square active region devices. The patterned magnetic stripe extends beyond the four-terminal active region by, respectively, an additional 5 or 10 squares. MR curves were taken with applied dc bias currents ranging from 0 to 70 mA and an ac excitation current of 10  $\mu$ A at 2 kHz. A single field coil provided a maximum magnetic field of 32 kA/m ( $\sim 400$  Oe) in the plane of the films, perpendicular to the long axis of the device strip and the bias current direction.

The MR curves in Fig. 1 show the appearance and evolution of multiple peaks in the magnetoresistance with increasing dc bias current. The lowest four curves constitute a family of MR curves versus bias current for a 16  $\mu$ m, 10-square, seven-layer annealed device. The curves are offset vertically to distinguish them; the lowest curve was obtained with no dc bias current. In the figure each higher curve rep-

resents an increase in bias current of 20 mA. The maximum in bias current displayed for the 16  $\mu$ m device, 60 mA, corresponds to a current density of  $8 \times 10^6$  A/cm<sup>2</sup>. The top two curves were obtained from an 8  $\mu$ m 20-square device on the same chip. The lower of the two 8  $\mu$ m MR curves was taken at roughly the same current density as the 60 mA 16  $\mu$ m MR curve. The MR response broadens roughly linearly with increasing bias current. A number of peaks appear at the higher bias currents and are especially apparent in the 8  $\mu$ m, 65 mA ( $1.6 \times 10^7$  A/cm<sup>2</sup>) MR curve. Their magnetic field positions also shift nearly linearly with bias current. For these devices, six peaks (numbered in Fig. 1 as 1,2,3,5,6,7) may be identified: The two negative field peaks (1,2) are easily discernible, two separate positive field peaks (6,7) may be distinguished at high currents, and two smaller bumps (3,5) appear on each side of zero field. We have also observed such peaks and peak shifts in five- and nine-layer unannealed structures. The number of peaks correlates with the number of layers: two on each side of the central maximum for the five-layer structure, three on each side for the seven-layer structure of Fig. 1, and four on each side for the nine layer system. The zero bias current curves are repeatable after high current bias, indicating that no irreversible changes have taken place within the structure.

Figure 2 illustrates how the positions of peaks from the seven-layer, 8  $\mu$ m, 20-square structure shift with bias current as determined from Lorentzian peak fits to the MR curves. Above 25 mA, their positions shift linearly with the bias current, suggesting that the peaks arise from a current-induced magnetic field inside the multilayer structure. Given the known resistivities of NiFe, Ag, and Ta, and a simple argument from Ampère's Law, we can estimate the values of the current-generated field strength<sup>1,1</sup> as  $H_I \approx Jz/2$  where  $z$  is the distance from the middle of the multilayer to the layer of interest and  $J$  is the current density. The lines in Fig. 2 plot the internal fields calculated versus current for each of the seven layers. These lines parallel the peak positions at high

<sup>a)</sup>Electronic mail: leif.kirschenbaum@colorado.edu

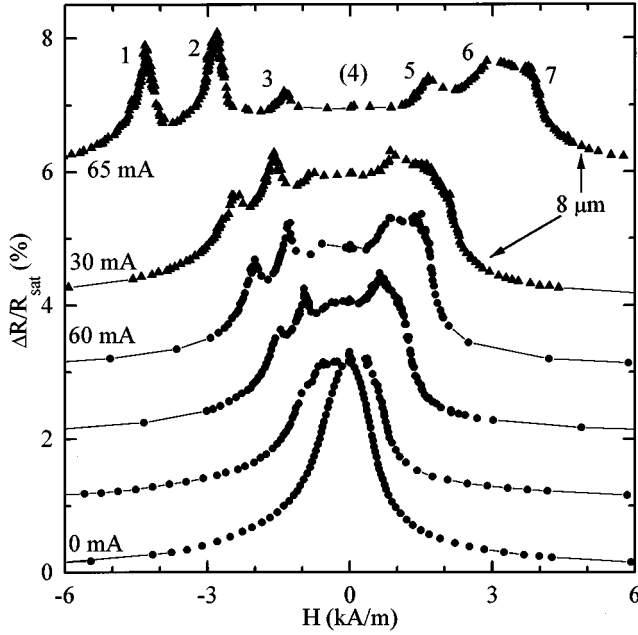


FIG. 1. Magnetoresistance curves from seven-layer annealed, 16  $\mu\text{m}$  wide, 10-square ( $\bullet$ ) and adjacent 8  $\mu\text{m}$  wide, 20-square devices ( $\blacktriangle$ ). The various 16  $\mu\text{m}$  curves were obtained at different bias currents in steps of 20 mA. For the 16  $\mu\text{m}$  device  $R_{\text{sat}} \approx 29 \Omega$ ; for the 8  $\mu\text{m}$  device  $R_{\text{sat}} \approx 59 \Omega$ . The peaks on the top curve are numbered starting from the magnetic layer closest to the substrate. Peak (4), though not resolved, represents a broad centered MR peak. It is required to fit the MR curve with seven Lorentzians. Curves are successively offset by 1% for clarity.

bias currents and effectively account for all the observed structures.

To illustrate the potential of these measurements for providing information about micromagnetic parameters, we describe the multilayer magnetic structure by means of an energy function similar to that used by Camley.<sup>2</sup> We include nearest-neighbor coupling terms, which arise from local magnetostatic interactions<sup>3</sup> and a Zeeman term:

$$E = \sum_{i=1}^{N-1} J_0 \cos(\theta_i - \theta_{i+1}) - \sum_{i=1}^N \mu_i H_i \cos \theta_i. \quad (1)$$

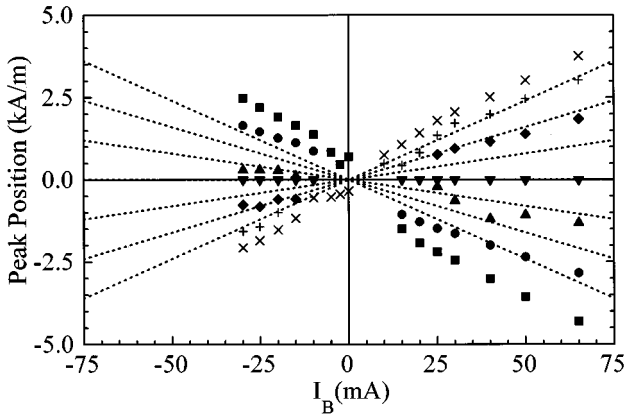


FIG. 2. Positions of the peaks in the magnetoresistance curves from the 8  $\mu\text{m}$  wide 20-square structure of Fig. 1. Peak positions are indicated both for positive and negative bias currents. Data for negative currents are truncated due to electric breakdown to the Si substrate for this polarity. Dotted lines indicate the calculated self fields at each NiFe layer in the multilayer.

Here,  $J_0$  is the magnetostatic coupling strength,  $\mu_i$  is the layer magnetic moment,  $H_i$  is the local field strength at layer  $i$ ,  $\theta_i$  is the angle of the  $i$ th moment with respect to the field direction, and  $N$  is the number of magnetic layers.  $H_i$  is a superposition of several field sources: we consider the externally applied field  $H_E$ , the internal current generated fields  $H_I$ , and any additional sources such as fields  $H_M$  arising from boundary magnetic charges. For our device geometry,  $H_E$  and  $H_I$  are in the plane of the device and perpendicular to the device current. At sufficiently large current densities,  $H_I$  can dominate the Zeeman term and the coupling term, causing the layer magnetizations to saturate parallel to  $H_I$ . Under these conditions, the layers above midplane are saturated in one direction, while those below are saturated antiparallel to the top layers. Then, there is one net antiferromagnetic interface in the system, with a “free” layer sandwiched in it, as illustrated schematically in the inset of Fig. 4. Application of an external field moves this interface up or down through the multilayer stack. The interface reaches a given layer position when the magnetostatic and Zeeman term on that layer balance to zero. Under high-current conditions minimization of Eq. (1) shows that the balance occurs at an external field strength such that:

$$H_{E,i} = H_I + \left( H_M + \alpha_i \frac{J_0}{\mu_i} \right) = m I_{\text{bias}} + y_0. \quad (2)$$

Here, we explicitly show the linear dependence of  $H_I$  on the bias currents (all other terms are collected in the factor  $m$ ) while  $y_0$  is the collection of bracketed terms.  $\alpha_i$  is the sum of the interaction strengths at the  $i$ th layer due to the local magnetostatic coupling from its neighbors; under the nearest-neighbor assumption of Eq. (1),  $\alpha_i = 1$  for the two outermost layers and zero for all other layers, since they have nearest neighbors which are antiparallel. If the interlayer coupling extends beyond nearest neighbors, then  $\alpha_i$  is nonzero for several or all layers and must be calculated.

In the standard GMR model, the interface between layers  $i$  and  $i+1$  contributes a resistance term proportional to  $\cos(\theta_i - \theta_{i+1})$ .<sup>2,4</sup> By adding these resistances in parallel under the assumption that all the saturated layers are rigidly pinned at either  $0^\circ$  or  $180^\circ$ , with only the balanced layer free to rotate, we find that there is no predicted change in the magnetoresistance until  $H_E$  is sufficient to drive the interface completely out of the system. This picture qualitatively explains the broadening of the MR curve with increasing bias current: Equation (2) predicts that the  $H_E$  necessary to bring the interface out of the last layer increases linearly with bias current. We have identified this broad flat magnetoresistance structure as the central peak (4) in Fig. 1. The additional sharp peaks which occur as the interface moves from layer to layer apparently arise from relaxation of the assumption of complete layer saturation. Equation (2) also implies that the finite intercepts of peak position versus bias current seen in Fig. 2 are related to  $J_0$ ,  $\mu_i$ , and  $H_M$ .

Figure 2 shows that there is a finite intercept for all but the central peak, consistent with Eq. (2). For the central peak we expect  $y_0 = 0$  due to the equal number of aligned and antialigned layers. For the other peaks there is net ferromagnetic alignment of the layers (finite  $H_M$ ) and possibly finite  $\alpha_i J_0$ . A linear fit to the high bias current peak positions

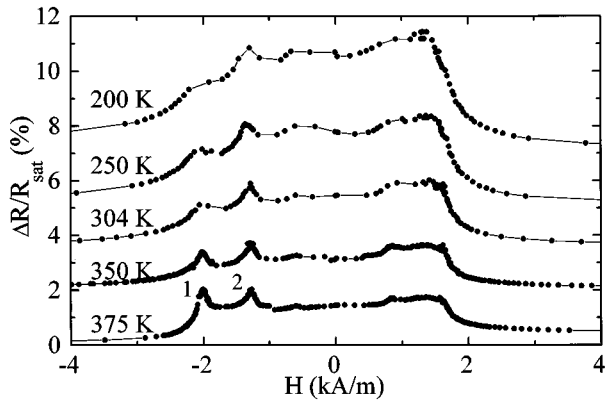


FIG. 3. Magnetoresistance curves with temperature as a parameter from the same 16  $\mu\text{m}$  wide structure as in Fig. 1. All curves were taken at 60 mA bias at various temperatures and are displaced by 1% successively.

yields an intercept  $y_0 = 0.8$  kA/m for the outermost peak. If the interlayer coupling term were the only term ( $H_M = 0$ ) and interactions were assumed to be nearest-neighbor ( $\alpha_i = 1$ ), then  $J_0/\mu$  would have a maximum value of 0.8 kA/m. Estimates of  $H_M$  due to the saturated magnetization  $M$ , of a single layer ( $\approx 2Mt/\pi w$ , where  $t$  is the thickness,  $w$  the width of the NiFe, and (Ref. 5)  $M \sim 835$  kA/m) indicate that  $H_M$  is smaller than our 0.8 kA/m intercept, strengthening our estimate of  $J_0/\mu$ . The outermost layer of a seven layer, 8  $\mu\text{m}$  wide device would experience a field  $H_M \sim 0.2$  kA/m. Traditionally,  $J_0/\mu$  is estimated from the half-width at half maximum of the zero bias current MR curve; we estimate  $J_0/\mu$  as 0.7 kA/m from the zero bias curve of Fig. 1, in good agreement with our value for  $J_0/\mu$  calculated from the outermost peak's zero-current intercept.

Significant information is also available from peak shapes. For example, while Eq. (2) implies that the high current MR curve should be symmetric with respect to zero external field, we find that the peaks on one side are significantly sharper than those on the other. Progressive roughening of the magnetic layers as we move higher up the thin-film stack causes inhomogeneity in  $H_I$  across the layer, implying roughness of 4 nm in the top layer position ( $\Delta z/z = \Delta H_I/H_I$ ), consistent with transmission electron micrographs which show top layer roughness  $\sim 5$  nm.

Figure 3 illustrates MR curves from the 16  $\mu\text{m}$ , 10-square structure with a bias current of 60 mA between 200 and 375 K. The peak positions do not change with temperature (determined from Lorentzian peak fits to the MR curves) and the total MR response increases with decreasing temperature, as has been reported for NiFe/Ag.<sup>6</sup> Figure 4 shows the width of the sharpest peaks, 1 and 2, of Fig. 3 as a function of temperature. They narrow with increasing temperature, likely due to a type of motional narrowing,<sup>7</sup> where metastable inhomogeneous magnetization configurations can be long-lived at low temperatures, leading to broader peaks due to the range of local magnetic configurations. Simple thermal arguments suggest for an equilibrium system of a moment  $\mu$  in a local induction field  $\mu_0 H_{\text{local}}$  ( $\mu_0$  is the permittivity of free space and  $H_{\text{local}}$  is the field at the moment  $\mu$ ) at temperature  $T$ , that alignment would occur when  $\mu(\mu_0 H_{\text{local}})/k_B T \approx 1$ , i.e., that the thermal width of a peak

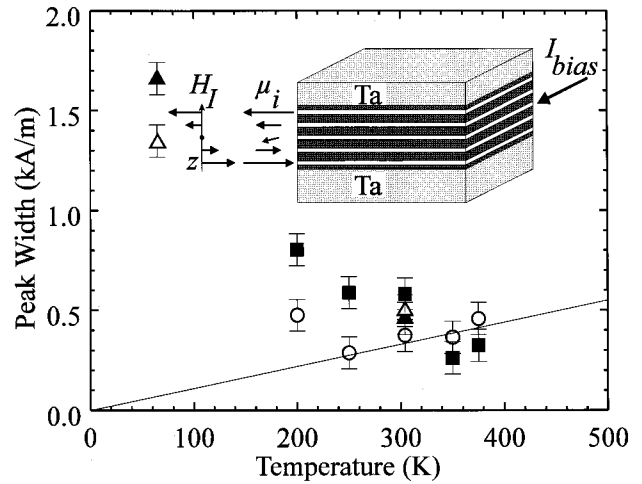


FIG. 4. Peak widths from the two sharp peaks of Fig. 3. (■) represents widths for the peak at  $-2.0$  kA/m, (○) the peak at  $-1.3$  kA/m. (Δ) represent widths of the sharp peaks from the 8  $\mu\text{m}$  device at 64 and 300 K. The solid line shows the peak broadening expected from a simple thermal model,  $\delta H \approx k_B T / \mu \mu$ , for a layer with moment  $\mu = 10^{-17}$  J/T  $\approx 10^6 \mu_B$ . The inset shows the orientation of the moments in a five-magnetic-layer device for  $H_B = 0$  and large  $H_I$  due to a bias current directed normal to the page. Layers above and below the midplane are oppositely saturated in and there is a single net antiferromagnetic interface.

would be roughly  $H \approx k_B T / \mu \mu_0$ . Taking the highest-temperature point of Fig. 4 for our narrowest peak, where the motional narrowing appears to be slowing down—perhaps as a prelude to the expected thermal broadening—we estimate the moment as  $\mu \approx 1 \times 10^{-17}$  J/T ( $\approx 1 \times 10^6 \mu_B$ , where  $\mu_B$  is the Bohr magneton). This result agrees well with values reported earlier<sup>8</sup> ( $3-4 \times 10^6 \mu_B$ ) for magnetic moments in these multilayers, derived from discrete resistance fluctuations. Our value of  $\mu$  allows an estimation of a domain volume of  $\sim 1 \times 10^5$  nm<sup>3</sup> or a domain of  $\sim 126$  nm radius and 2 nm thickness. Using our values for  $\mu$  and  $J_0/\mu$  we estimate that this pancake sees an interlayer coupling  $J_0 \sim 1 \times 10^{-20}$  J ( $0.07$  eV  $= k_B \times 700$  K).

These high current density induced peaks in the MR curves provide new ways to measure a variety of micromagnetic parameters. The self-field effects permit the selection of a particular “free” layer in a multilayer by balancing externally applied field against internal field. This ability to separate out one layer at a time in a multilayer stack should prove useful in further understanding the micromagnetics of such structures.

<sup>1</sup> Y. K. Kim and S. C. Sanders, Appl. Phys. Lett. **66**, 1009 (1995).

<sup>1.1</sup> N. Smith, IEEE Trans. Magn. **30**, 3822 (1994).

<sup>2</sup> R. E. Camley, J. Phys. C **5**, 3727 (1993).

<sup>3</sup> J. C. Slonczewski, J. Magn. Magn. Mater. **129**, L123 (1994).

<sup>4</sup> A. Chaiken, G. A. Prinz, and J. J. Krebs, J. Appl. Phys. **67**, 4892 (1990).

<sup>5</sup> R. A. McCurrie, *Ferromagnetic Materials Structure and Properties* (Academic, New York, 1994), p. 34.

<sup>6</sup> B. Rodmacq, G. Palumbo, and Ph. Gerard, J. Magn. Magn. Mater. **118**, L11 (1993).

<sup>7</sup> A. Abragam, *Principles of Nuclear Magnetism* (Oxford, New York, 1961), Chap. X.

<sup>8</sup> L. S. Kirschenbaum, C. T. Rogers, S. E. Russek, and S. C. Sanders, IEEE Trans. Magn. **31**, 3943 (1995).